Novel observation of isospin structure of short-range correlations in Calcium isotopes

D. Nguyen,[1,2] Z. Ye,[3,1] P. Aguilera,[4] Z. Ahmed,[5] H. Albataineh,[6] K. Allada,[7] B. Anderson,[8] D. Anez,[9] K. Aniol,[10] J. Annand,[11] J. Arrington,[3] T. Averett,[12] H. Baghdasaryan,[1] X. Bai,[13] A. Beck,[14] S. Beck,[14] V. Bellini,[15] F. Benmokhtar,[16] A. Camsonne,[7] C. Chen,[17] J.-P. Chen,[7] K. Chirapatpimol,[1] E. Cisbani,[18] M. M. Dalton,[1,7] A. Daniel,[19] D. Day,[1] W. Deconinck,[2] M. Defurne,[20] D. Flay,[21] N. Fomin,[22] M. Friend,[23] S. Frullani,[18] E. Fuchey,[21] F. Garibaldi,[18] D. Gaskell,[7] S. Gilad,[2] R. Gilman,[24] S. Glamazdin,[25] C. Gu,[1] P. Guèye,[17] C. Hanretty,[1] J.-O. Hansen,[7] M. Hashemi Shabestari,[1] D. W. Higinbotham,[7] M. Huang,[26] S. Iqbal,[10] G. Jin,[1] N. Kalantarians,[1] H. Kang,[27] A. Kelleher,[2] I. Korover,[28] J. LeRose,[7] J. Leckey,[29] S. Li,[30] R. Lindgren,[1] E. Long,[8] J. Mammei,[31] D. J. Margaziotis,[10] P. Markowitz,[32] D. Meekins,[7] Z. Meziani,[21] R. Michaels,[7] M. Mihovilovič,[33] N. Muangma,[2] C. Munoz Camacho,[34] B. E. Norum,[1] Nuruzzaman,[35] K. Pan,[2] S. Phillips,[30] E. Piasetzky,[28] I. Pomerantz,[28,36] M. Posik,[21] V. Punjabi,[37] X. Qian,[26] Y. Qiang,[7] X. Qiu,[38] P. E. Reimer,[3] A. Rakhman,[5] S. Riordan,[1,39] G. Ron,[40] O. Rondon-Aramayo,[1] A. Saha,[7,*] L. Selvy,[8] A. Shahinyan,[41] R. Shneor,[28] S. Širca,[42,33] K. Slifer,[30] P. Solvignon,[30,7,*] N. Sparveris,[21] R. Subedi,[1] V. Sulkosky,[2] D. Wang,[1] J. W. Watson,[8] L. B. Weinstein,[6] B. Wojtsekhowski,[7] S. A. Wood,[7] I. Yaron,[28] X. Zhan,[3] J. Zhang,[7] Y. W. Zhang,[24] B. Zhao,[12] X. Zheng,[1] P. Zhu,[43] and R. Zielinski[30]

(The Jefferson Lab Hall A Collaboration)

[1] *University of Virginia, Charlottesville, Virginia 22904*
[2] *Massachusetts Institute of Technology, Cambridge, Massachusetts 02139*
[3] *Physics Division, Argonne National Laboratory, Argonne, Illinois 60439*
[4] *Institut de Physique Nucléaire (UMR 8608), CNRS/IN2P3 - Université Paris-Sud, F-91406 Orsay Cedex, France*
[5] *Syracuse University, Syracuse, New York 13244*
[6] *Old Dominion University, Norfolk, Virginia 23529*
[7] *Thomas Jefferson National Accelerator Facility, Newport News, Virginia 23606*
[8] *Kent State University, Kent, Ohio 44242*
[9] *Saint Mary's University, Halifax, Nova Scotia, Canada*
[10] *California State University, Los Angeles, Los Angeles, California 90032*
[11] *University of Glasgow, Glasgow G12 8QQ, Scotland, United Kingdom*
[12] *College of William and Mary, Williamsburg, Virginia 23187*
[13] *China Institute of Atomic Energy, Beijing, China*
[14] *Nuclear Research Center Negev, Beer-Sheva, Israel*
[15] *Universita di Catania, Catania, Italy*
[16] *Duquesne University, Pittsburgh, Pennsylvania 15282*
[17] *Hampton University, Hampton, Virginia 23668*
[18] *INFN, Sezione Sanità and Istituto Superiore di Sanità, 00161 Rome, Italy*
[19] *Ohio University, Athens, Ohio 45701*
[20] *CEA Saclay, F-91191 Gif-sur-Yvette, France*
[21] *Temple University, Philadelphia, Pennsylvania 19122*
[22] *University of Tennessee, Knoxville, Tennessee 37996*
[23] *Carnegie Mellon University, Pittsburgh, Pennsylvania 15213*
[24] *Rutgers, The State University of New Jersey, Piscataway, New Jersey 08855*
[25] *Kharkov Institute of Physics and Technology, Kharkov 61108, Ukraine*
[26] *Duke University, Durham, North Carolina 27708*
[27] *Seoul National University, Seoul, Korea*
[28] *Tel Aviv University, Tel Aviv 69978, Israel*
[29] *Indiana University, Bloomington, Indiana 47405*
[30] *University of New Hampshire, Durham, New Hampshire 03824*
[31] *Virginia Polytechnic Inst. and State Univ., Blacksburg, Virginia 24061*
[32] *Florida International University, Miami, Floria 33199*
[33] *Jozef Stefan Institute, Ljubljana, Slovenia*
[34] *Université Blaise Pascal/IN2P3, F-63177 Aubière, France*
[35] *Mississippi State University, Starkville, Mississippi 39762*
[36] *The University of Texas at Austin, Austin, Texas 78712*
[37] *Norfolk State University, Norfolk, Virginia 23504*
[38] *Lanzhou University, Lanzhou, China*
[39] *University of Massachusetts, Amherst, Massachusetts 01006*
[40] *Racah Institute of Physics, Hebrew University of Jerusalem, Jerusalem, Israel*
[41] *Yerevan Physics Institute, Yerevan 375036, Armenia*
[42] *Faculty of Mathematics and Physics, University of Ljubljana, Ljubljana, Slovenia*
[43] *University of Science and Technology, Hefei, China*

(Dated: April 7, 2020)

Short Range Correlations (SRCs) have been identified as being responsible for the high momentum tail of the nucleon momentum distribution, n(k). Hard, short-range interactions of nucleon pairs generate the high momentum tail and imprint a universal character on n(k) for all nuclei at large momentum. Triple coincidence experiments have shown a strong dominance of np pairs, but these measurements involve large final state interactions. This paper presents the results from Jefferson Lab experiment E08014 which measured inclusive electron scattering cross-section from Ca isotopes. By comparing the inclusive cross section from ^{48}Ca to ^{40}Ca in a kinematic region dominated by SRCs we provide a new way to study the isospin structure of SRCs.

PACS numbers: 13.60.Hb, 25.10.+s, 25.30.Fj

The naïve nuclear shell model has guided our understanding of nuclear properties for 60 years and it is still appealing as a predictive and illustrative nuclear model. This model, with nucleons moving in an average (mean-field) generated by the other nucleons in the nucleus, provides a quantitative account of a large body of nuclear properties. These include shell closures ("magic numbers"), the foundation of which is the appearance of gaps in the spectrum of single-particle energies [1].

The shell model is not without certain deficits which arise from what are generally called correlations - effects that are beyond mean field theories such as long-range correlations associated with collective phenomena: giant resonances, vibrations and rotations. In addition, electron-nucleus scattering experiments have unambiguously shown large deviations from the shell model predictions, arising from the occurrence of strong short-range nucleon-nucleon correlations. These two-nucleon SRCs (2N-SRC) move particles from the shell model states to large excitation energies and generate a high-momentum tail in the single particle momentum distribution. Consequently, over large range of A the number of protons found in the valence shells orbitals is significantly less than expected, typically 60%–70% of the predicted shell model occupancy [2].

Inclusive experiments are able to isolate the 2N-SRC through selective kinematics: working at large momentum transfer ($Q^2 \geq 1.5$ GeV^2) and small energy transfer ($\nu \leq \frac{Q^2}{2m}$), corresponding to $x = \frac{Q^2}{2m\nu} > 1$, where m is the mass of the proton. In this region, it is kinematically impossible for mean field nucleons to contribute and where competing inelastic processes are minimized [3–5]. It was through inclusive experiments [6–8] that 2N-SRCs were first revealed by the appearance of predicted plateaus [3] in the A/^{2}H per-nucleon cross section ratio of nuclei to the deuteron. The height of the plateau is related to probability of finding a 2N-SRC in nucleus A, relative to the deuteron, indicating that ∼20% of the protons and neutrons in medium-to-heavy mass nuclei have momenta greater than the Fermi momentum $k_F \simeq 250$ MeV [7]. The bulk of these nucleons do not arise in a shell model description as they are the result of brief short-range interaction among pairs of nucleons giving rise to large relative momenta and modest center-of-mass motion, $k_{CM} < k_F$ [3].

The isospin dependence of 2N-SRCs has been determined via A$(p, p'pN)$ [9] and A$(e, e'pN)$ [10–12] reactions in which the scattered particle (either a proton or an electron) is measured in coincidence with a high-momentum proton whose initial momentum, reconstructed assuming plane wave scattering, is approximately opposite that of the second high-momentum nucleon.

These measurements exhibit a dominance of np pairs over pp pairs for initial nucleon momenta of 300-600 MeV which has been traced to the tensor part of the NN interaction [13–16]. These triple-coincidence experiments are sensitive to the isospin structure of the SRC through direct measurement of the final state nucleons. Because the signature of large back-to-back momenta is also consistent with striking a low-momentum nucleon which rescatters, there are large contributions from final state interactions (including charge exchange) that need to be accounted for in comparing pp and np pairs [10–12]. Isospin dependence has never been established in inclusive scattering, A(e, e') until now.

We present here new A(e, e') measurements performed as part of Jefferson Lab experiment E08-014 [17]. Initial results on the search for three-nucleon SRCs in helium isotopes were published in Ref. [18]. This work focused on a measurement of the isospin dependence of 2N-SRCs in the cross section ratio of scattering from ^{48}Ca and ^{40}Ca. The excess neutrons in ^{48}Ca change the relative ratio of potential pp, np, and nn pairs, yielding a different isospin distribution of high-momentum pairs differently for isospin-independent SRCs and np-dominated SRCs. This can be seen in a simple estimate for the two cases. As a starting point, we take the fraction of nucleons in SRCs to be identical for these two targets, based on the observation of an A-independent value of a_2, the A/^{2}H cross section ratio for $1.5 < x < 2$, for heavy nuclei [6, 8]. In the case of isospin-independent SRCs, protons and neutrons will have the same probability of appearing at momenta above k_F, giving a cross section ratio of $\frac{\sigma_{^{48}Ca}/48}{\sigma_{^{40}Ca}/40} = \frac{(20\sigma_{ep}+28\sigma_{en})/48}{(20\sigma_{ep}+20\sigma_{en})/40} \approx 0.93$ taking $\sigma_{ep}/\sigma_{en} \approx 2.5$, corresponding to the kinematics of this experiment. If SRCs are dominated by np pairs, the cross section ratio would be unity for isoscalar nuclei and slightly lower for non-isoscalar nuclei (see also [19, 20]).

Jefferson Lab experiment E08-014 [17] ran during the Spring of 2011. A 3.356 GeV continuous wave electron beam was directed onto a variety of targets, including ^{2}H, ^{3}He, ^{4}He, ^{12}C and targets of natural calcium (mainly ^{40}Ca) and an enriched target of 90.04% ^{48}Ca (referred to as the ^{40}Ca and ^{48}Ca targets, respectively). The scattered electrons were detected at angles of θ=21°, 23°, 25°, and 28°, though no Calcium data was taken at 28°. The data presented here cover a kinematic region of $1.3 < Q^2 < 1.9$ GeV^2 and $1 < x < 3$.

The inclusive scattered electrons were detected using two nearly identical left and right high resolution spectrometers (LHRS and RHRS). Each spectrometer was equiped with a detector package consisting of of two vertical drift chambers (VDC) for tracking information, a Gas Cerenkov counter and two layers of lead glass calorimeters for particle identification (PID), and two scintillator counter planes for triggering [21].

The accumulated charge for each experimental run was measured by beam current monitors (BCMs) with an uncertainty of 0.5%. The dead-time due to the inability of the data acquisition system to accept new triggers while processing the current event was corrected for each run using the trigger scaler information. The main trigger for data collection requires a coincidence of signals from two scintillator planes and the Cerenkov, which had a local inefficiency. The Cerenkov efficiency was calculated as a function of x and applied to the measured yield for each bin. Pions were rejected (with negligible remaining pion contamination) by applying additional software cuts on both the Cerenkov counter and the lead glass calorimeter with efficiencies of 99.5% and 99.6% respectively, with a tracking efficiency of 98.5%. Detailed descriptions of the experimental setup and data analysis can be found in [22] and [23].

The angle and momentum of the scattered electron at the reaction vertex were reconstructed from the detected track at the VDCs using a set of optics matrices. The optics from another experiment [24], having the identical magnetic tune as this experiment, was used for the LHRS. The tune for the RHRS had to be modified because the third quadrupole couldn't run at the required field, and lack of a complete set of optics data led to a reduced resolution in the RHRS. The reduced resolution impacts the extraction of the cross section at large x values where the cross section falls extremely rapidly, requiring larger correction. Because the RHRS was typically taking data in the same kinematics as the LHRS, we use only the data from the LHRS except for the 21° data, where the largest x values were measured only in the RHRS. For this setting we include the ratios from the RHRS, as the smearing has a negligible impact on the cross section ratios in the region where the ratio is flat.

The yield for the experiment is simulated using a detailed model of the HRS optics and acceptance, with events generated uniformly and weighted by a radiative cross section model [23, 25]. The model uses a y-scaling fit [26, 27] for quasi-elastic cross section (initially based on previous data, and iteratively updated to match the extracted cross sections from this experiment) and a global fit [28] for the inelastic contribution. The Born cross section is extracted by taking the model cross section and correcting it by the ratio of measured to simulated yield. Comparing the results extracted with the final model and the model before being adjusted to match our data indicates a model uncertainty of 0.5% in both the absolute cross sections and the target ratios.

The cross section ratio obtained from the enriched and natural Calcium targets are then corrected to yield ^{48}Ca/^{40}Ca ratio, based on the isotopic analysis of the targets. No correction was applied to the natural Calcium, while the enriched Calcium target had a 9.96% contribution of ^{40}Ca and 90.04% ^{48}Ca (by number of atoms). Thus, the cross section for ^{48}Ca was obtained by correcting the enriched Ca target data using the measured ^{40}Ca cross sections; the correction is typically 2%.

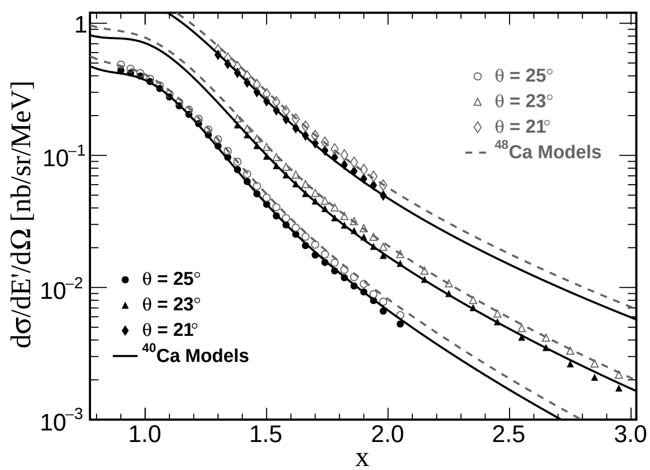

FIG. 1. ^{48}Ca and ^{40}Ca cross sections for three different angle settings, along with the cross section model used in the analysis. Uncertainties shown include statistical and point-to-point systematic uncertainties; an additional normalization uncertainty of 2.7% for ^{40}Ca and 3.0% for ^{48}Ca is not shown.

The measured Calcium cross sections are presented in Figure 1. For the cross sections, the point-to-point systematic uncertainty is estimated to be 1.9%, with dominant contributions coming from the acceptance (1.5%), radiative corrections (1%), and the model dependence of the cross section extraction (0.5%). In addition, there is an overall normalization uncertainty of 2.7%, coming mainly from the acceptance (2%), radiative correction (1%), and target thickness (1%). These are the uncertainties for the ^{40}Ca target, while the dilution correction used to extract the ^{48}Ca cross section increases these, giving a 2.1% point-to-point and a 3.0% normalization uncertainty.

The per nucleon cross-section ratio of ^{48}Ca to ^{40}Ca

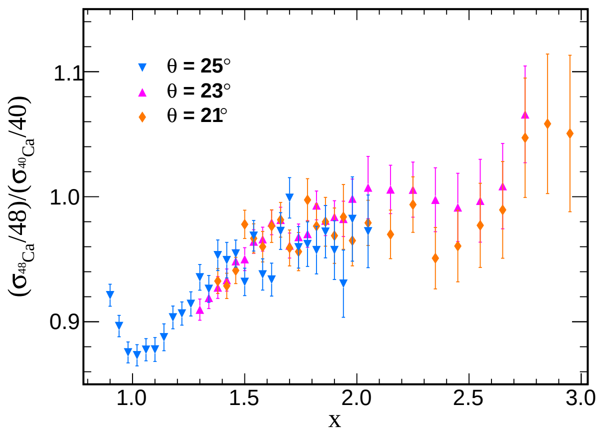

FIG. 2. Ratio of the cross section per nucleon for ^{48}Ca and ^{40}Ca for three scattering angles. Uncertainties shown include statistical and point-to-point systematic uncertainties; an additional normalization uncertainty of 1% is not shown.

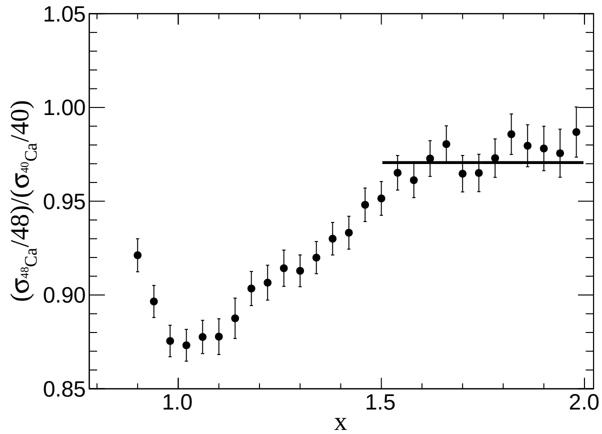

FIG. 3. Ratio of the cross section per nucleon for ^{48}Ca and ^{40}Ca combining all three data sets. A 1% normalization uncertainty is not shown. The line indicates the fit for the cross section ratio in the SRC region

is presented in Figure 2 for each of the three scattering angles and in Figure 3 after combining of the data sets. Because the cross section and experimental conditions are very similar for the two targets, many of the uncertainties in the cross sections cancel or are reduced in the ratio. The systematic uncertainty on the ratios is 0.9%, dominated by the model dependence in the extraction (0.5%), measurement of the beam charge (0.5%) and the radiative correction (0.5%). An additional 1% normalization uncertainty, associated with the uncertainty in the relative target thicknesses, is not shown. When combining the angles for Fig. 3, we combine the statistics of the individual sets and then apply the 0.9% point-to-point uncertainty (and 1% normalization uncertainty) to the combined result.

Note that the rise from $x = 1$ to $x = 1.6$ looks slightly different from previously observed A/^{2}H ratios. This is expected as the shape in the A/^{2}H ratios is driven by the deuterium cross section, which is narrowly peaked at and roughly symmetric about x=1. The line in Fig. 3 indicates the value of R_{SRC}, the average in the plateau region: $1.5 < x < 2$. The fit gives $R = 0.971(3)(6)(10) = 0.971(12)$ where the error contributions come from the point-to-point uncertainties, the cut dependence of the extracted R_{SRC}, and the normalization uncertainty of the ratios. The cut dependence is taken to be the RMS scatter of R_{SRC} values fit separately to the three scattering angles for three different minimum x values, $x_{min} = 1.5, 1.6$ and 1.7.

The observed value of R_{SRC} is between the predictions for isospin independence ($R_{\mathrm{SRC}} \approx 0.93$) and total np dominance ($R_{\mathrm{SRC}} \approx 1$) and provides an independent confirmation of the enhancement of np pairs in SRCs.

To interpret this ratio in terms of relative np, pp, and nn SRC contributions, and to compare these results to observables from previous measurements, we use a simple model to estimate the inclusive, exclusive, and two-nucleon knockout ratios in terms of a few parameters. We take the number of 2N-SRCs to be a product of the number of total pairs, the probability for any two nucleons to be close enough together to interact via the short-range NN interaction (f_{sr}), and the probability that the NN interaction generates a high-momentum pair (p_{NN}). The total number of np, pp, and nn pairs are NZ, $Z(Z-1)/2$, and $N(N-1)/2$, respectively. The fraction of nucleons at short distance, f_{sr}, depends on the nucleus and is assumed to be identical for nn, np, and pp pairs. The probability that these nucleons generate high momentum pairs, p_{np} and $p_{pp} = p_{nn}$, depends on the momentum range of the initial nucleons, ΔP_i, defined by the experiment for coincidence measurements or by the kinematics in inclusive scattering. Given this, we can express the number of np and pp SRCs as:

$$N_{np} = NZ \cdot f_{sr}(A) \cdot p_{np}(\Delta P_i) \tag{1}$$

$$N_{pp} = Z(Z-1)/2 \cdot f_{sr}(A) \cdot p_{pp}(\Delta P_i) \tag{2}$$

While p_{np} and p_{pp} may depend strongly on ΔP_i, we assume that their ratio has a much weaker dependence, as observed in Ref. [12], and so their ratio extracted from different measurements should be qualitatively comparable. This leaves only $f_{sr}(A)$ as an unknown. In comparing different observables on the same nucleus, e.g. taking the ratio of A(e,e'pp) to A(e,e'pn), $f_{sr}(A)$ cancels out. In the limit of large nuclei, any given nucleon will be sensitive to short-range interactions with nucleons in some fixed volume, while the number of nucleons grows with A, suggesting that $f_{sr}(A)$ should scale as $1/A$. With this assumption, our model produces a constant value of a_2

for heavy isoscalar nuclei, consistent with the observation of approximate saturation [29].

Using this simple approach, we can calculate the number of *pp*, *np*, and *nn* pairs in the targets, and then weigh this by the cross section for elastic scattering from the two nucleons in each pair to obtain the inclusive cross section in the SRC region for each target. In taking the ratio of these cross sections, the overall scale of $f_{sr}(A)$ drops out and only the A-dependence remains, and the cross section ratio can then be written in terms of the ratio of p_{np} to p_{pp}, the enhancement factor of *np* pairs to high momentum relative to *pp* and *nn* pairs. Given the value of σ_{ep}/σ_{en}, taken to be 2.55-2.60 for these kinematics, this model predicts the cross section ratio to be 0.93 for isospin independence, and 0.972 for np dominance. The np-dominance prediction is slightly below unity; the model predicts that for an isoscalar nucleus, the fraction of np-SRCs, and thus the cross section per nucleon, would be identical for heavy nuclei. Because ^{48}Ca has $20 \cdot 28$ potential NP pairs, rather than $24 \cdot 24$ for an isoscalar A=48 nucleus, the ratio is suppressed by a factor of $(20 \cdot 28)/(24 \cdot 24) = 0.972$. Thus, the observed cross section ratio of 0.971(12) corresponds to almost complete *np* dominance. Taking into account its uncertainty, we find that $p_{np}/p_{pp} > 2.9$ at the 95% confidence level, and $p_{np}/p_{pp} > 1.6$ at the 99% confidence level, demonstrating *np* dominance using the isospin structure of the target, rather than the detected nucleons, to study the isospin structure.

Note that the ratio p_{np}/p_{pp} is not directly comparable to the enhancement factor of ∼10 obtained in triple coincidence experiments [11, 12], as it removes the contribution from simple pair counting. For example, ^{4}He has four *np* pairs and only one *pp* pair, and thus one would expect *np* pairs to dominate, even if the generation of high-momentum pairs had no isospin dependence. However, we can use this simple model to extract p_{np}/p_{pp} from other measurements, A(e,e'pp)/A(e,e'pn) or A(e,e'p)/A(e,e'n), using the same assumptions as made above. As noted above, p_{np} and p_{pp} depend on the momentum of the struck nucleon in the initial-state SRC, while for the inclusive case, they correspond to an average over the range probed in the scattering which depends on Q^2 and the x range of the data. Because of this, the extracted enhancement factor for inclusive scattering corresponds to a range of momenta that should be similar, but not identical, to the momentum range selected in the coincidence knockout reactions.

Writing out the ratio of A(e,e'pp)/A(e,e'pn) in terms of p_{np}/p_{pp} allows us to take the observed ratios and extract the np enhancement factor. For ^{4}He [12], the pp/np fraction is (5.5±3)%, yielding a one-sigma range of $2.9 < p_{np}/p_{pp} < 10$. For ^{12}C, the pp/np fraction is (5.6±1.8)% yielding $5.6 < p_{np}/p_{pp} < 11$. The full expressions are provided in the supplementary material. These correspond to the lowest P_m bins for the triple-coincidence measurements, P_m from roughly 400-600 MeV/c, to more closely match the main contributions to the inclusive measurement. As noted above, these values are not exactly equivalent to the values extracted from the inclusive scattering, but they paint a consistent picture of significant *np* dominance in SRCs over a range of light and heavy nuclei. In conclusion, the per nucleon cross section ratio of ^{48}Ca/^{40}Ca is consistent with significant np dominance in the creation of SRCs. It shows an enhancement of np pairs over pp pairs at more than the three sigma level.

This data provides the first evidence of *np* dominance from inclusive scattering, making use of the isospin structure of the target rather than the final NN pair. This approach avoids the significant corrections required to interpret triple-coincidence measurements, but does not provide a good quantitative measure of the enhancement factor because of the small difference between isospin-independent and np-dominance pictures. A recent experiment measured the inclusive ratio for scattering from ^{3}H and ^{3}He, which is significantly more sensitive to the isospin structure of the SRCs [30]. In this case, the ^{3}H/^{3}He cross section ratio is approximately 0.75 for isospin independence and 1 for np dominance, giving roughly five times more sensitivity than the ^{48}Ca/^{40}Ca ratio, without having to make any assumption about the A dependence of $f_{sr}(A)$ in comparing the two nuclei. A measurement of this cross section ratio with comparable uncertainties should provide the best quantitative measurement of the enhancement of np pairs at high momentum.

We acknowledge the outstanding support from the Jefferson Lab Hall A technical staff and the JLab target group. This work was supported in part by the DOE Office of Science, Office of Nuclear Physics, under contracts DE-AC02-06CH11357 and DE-FG02-96ER40950, and the National Science Foundation, and under DOE contract DE-AC05-06OR23177, under which JSA, LLC operates JLab. The ^{48}Ca isotope used in this research was supplied by the Isotope Program within the Office of Nuclear Physics in the Department of Energys Office of Science. Experiment E08-014 was developed by Patricia Solvignon whose passing is still mourned by our community.

* deceased

[1] E. Caurier, G. Martinez-Pinedo, F. Nowacki, A. Poves, and A. P. Zuker, Rev. Mod. Phys. **77**, 427 (2005).
[2] J. Kelly, Adv. Nucl. Phys. **23**, 75 (1996).
[3] L. Frankfurt and M. Strikman, Physics Reports **76**, 215 (1981).
[4] M. M. Sargsian *et al.*, J. Phys. **G29**, R1 (2003).
[5] J. Arrington, D. Higinbotham, G. Rosner, and M. Sargsian, Prog. Part. Nucl. Phys. **67**, 898 (2012).

[6] L. L. Frankfurt, M. I. Strikman, D. B. Day, and M. Sargsyan, Phys. Rev. C **48**, 2451 (1993).
[7] K. S. Egiyan *et al.*, Phys. Rev. **C 68**, 014313 (2003).
[8] N. Fomin *et al.*, Phys. Rev. Lett. **108**, 092502 (2012).
[9] A. Tang *et al.*, Phys. Rev. Lett. **90**, 042301 (2003).
[10] Jefferson Lab Hall A, R. Shneor *et al.*, Phys. Rev. Lett. **99**, 072501 (2007).
[11] R. Subedi *et al.*, Science **320**, 1476 (2008).
[12] I. Korover *et al.*, Phys. Rev. Lett. **113**, 022501 (2014).
[13] R. Schiavilla, R. B. Wiringa, S. C. Pieper, and J. Carlson, Phys. Rev. Lett. **98**, 132501 (2007).
[14] M. Alvioli, C. Ciofi degli Atti, and H. Morita, Phys. Rev. Lett. **100**, 162503 (2008).
[15] R. B. Wiringa, R. Schiavilla, S. C. Pieper, and J. Carlson, Phys. Rev. **C 78**, 021001 (2008).
[16] R. Wiringa, R. Schiavilla, S. C. Pieper, and J. Carlson, Phys. Rev. **C 89**, 024305 (2014).
[17] J. Arrington, D. Day, D. Higinbotham, and P. Solvignon, Three-nucleon short range correlations studies in inclusive scattering for $0.8 < Q^2 < 2.8 (GeV/c)^2$, http://hallaweb.jlab.org/experiment/E08-014/, 2011.
[18] Z. Ye *et al.*, Phys. Rev. **C 97**, 065204 (2018).
[19] M. Vanhalst, W. Cosyn, and J. Ryckebusch, Phys. Rev. **C 84**, 031302 (2011).
[20] M. Vanhalst, J. Ryckebusch, and W. Cosyn, Phys. Rev. **C 86**, 044619 (2012).
[21] J. Alcorn *et al.*, Nucl. Instrum. Meth. **A522**, 294 (2004).
[22] D. Nguyen, Ph.D Thesis, University of Virginia, 2019.
[23] Z. Ye, Ph.D Thesis, University of Virginia, 2013, arXiv:1408.5861.
[24] B.Wojtsekhowski, J. Arrington, M. E. Christy, S. Gilad, and V. Sulkosky, Precision measurement of the proton elastic cross section at high q^2, Jefferson Lab Experiment Proposal E12-07-108, 2007.
[25] XEMC: Quasielastic Cross Section Model, https://www.jlab.org/∼yez/XEMC/.
[26] G. B. West, Physics Reports **18**, 263 (1975).
[27] D. B. Day, J. S. McCarthy, T. W. Donnelly, and I. Sick, Annual Review of Nuclear and Particle Science **40**, 357 (1990).
[28] P. E. Bosted and V. Mamyan, (2012), arXiv:1203.2262.
[29] J. Arrington *et al.*, Phys. Rev. **C 86**, 065204 (2012).
[30] J. Arrington, D. Day, D. W. Higinbotham, and P. Solvignon, Precision measurement of the isospin dependence in the 2N and 3N short range correlation region, Jefferson Lab Experiment Proposal E12-11-112, 2011.